

Chronic iron overload enhances inducible nitric oxide synthase expression in rat liver

Pamela Cornejo ^a, Patricia Varela ^b, Luis A. Videla ^a, Virginia Fernández ^{a,*}

^a Programa de Farmacología Molecular y Clínica, Instituto de Ciencias Biomédicas, Facultad de Medicina, Universidad de Chile, Casilla 70000, Santiago-7, Chile

^b Programa de Biología Celular y Molecular, Instituto de Ciencias Biomédicas, Facultad de Medicina, Universidad de Chile, Casilla 70000, Santiago-7, Chile

Abstract

Iron is an essential micronutrient promoting oxidative stress in the liver of overloaded animals and human, which may trigger the expression of redox-sensitive genes. We have tested the hypothesis that chronic iron overload (CIO) enhances inducible nitric oxide synthase (iNOS) expression in rat liver by extracellular signal-regulated kinase (ERK1/2) and NF- κ B activation. CIO (diet enriched with 3%(wt/wt) carbonyl-iron for 12 weeks) increased liver protein carbonylation and decreased reduced glutathione (GSH) content and the GSH/GSSG ratio after 6 weeks, parameters that are normalized after 8–12 weeks of treatment. These changes are paralleled by higher phosphorylated-ERK1/2 to non-phosphorylated-ERK1/2 ratios at 6 and 8 weeks, increased NF- κ B DNA binding to the iNOS gene promoter at 8–12 weeks, and higher iNOS mRNA expression and activity at 8 and 12 weeks. It is concluded that CIO triggers liver oxidative stress at early times, with upregulation of iNOS expression involving the ERK/NF- κ B pathway at later times, a finding that may represent a hepatoprotective mechanism against CIO toxicity in addition to the recovery of GSH homeostasis.

Keywords: Chronic iron overload; Liver oxidative stress; Inducible nitric oxide synthase expression

Iron is the most abundant transition metal in the body that is mainly present in protein-bound forms such as heme and non-heme proteins, playing a major role in electron transfer and oxygen utilization [1]. This transition metal promotes free radical generation through Fenton and/or Haber–Weiss reactions, thus triggering secondary chain reactions in the oxidative modification of lipids, proteins, and DNA in different organs including the liver, the main site for iron metabolism [2]. Chronic iron overload (CIO) produces liver oxidative stress through an increased rate of hydroxyl radical (HO \cdot) generation, which may lead to lysosomal,

mitochondrial, and microsomal damage, resulting in organelle dysfunction [3]. In addition to direct cellular oxidant injury, reactive oxygen (ROS) and nitrogen (RNS) species may constitute signals regulating (i) protein function through reversible oxidation and/or nitrosation of protein sulfhydryls [4] or (ii) gene expression, in the different cell-types of the hepatic sinusoid [5,6], through mechanisms involving ROS and lipid oxidation products of ROS-dependent reactivity that activate kinases, phosphatases, and/or redox-sensitive transcription factors [7,8].

Nitric oxide (\cdot NO) is an inorganic RNS synthesized in liver by inducible nitric oxide synthase (iNOS) found in hepatocytes, Kupffer cells, and endothelial cells [9], whose expression is controlled by the redox-sensitive transcription factor NF- κ B [10]. A number of studies

* Corresponding author. Fax: +56 2 7372783.

E-mail address: vfernand@med.uchile.cl (V. Fernández).

have described the complex interrelationships between iron and $\cdot\text{NO}$ [11,12], which can result in changes in $\cdot\text{NO}$ production in vivo. Increased $\cdot\text{NO}$ generation has been evidenced in the liver under conditions of acute iron overload [13]. These data are in accordance with the higher expression of liver iNOS described in patients with hereditary hemochromatosis [14], and with the enhancement in $\cdot\text{NO}$ production induced by iron in cultured proximal tubule cells [15], an effect that is mediated by increased NF- κ B DNA binding activity [16]. Furthermore, in vivo studies showed that the renal expression of eNOS and iNOS in the rat is elevated after iron overload [17], whereas saccharated colloidal iron enhanced the LPS-dependent production of $\cdot\text{NO}$ and induced iNOS in Kupffer cells [18]. In view of these considerations, the aim of this study was to test the hypothesis that CIO upregulates the expression of iNOS and NOS activity in conditions of liver oxidative stress, through a cascade involving the activation of the extracellular signal-regulated kinase (ERK) pathway and increased NF- κ B DNA binding to the iNOS gene. For this purpose, phosphorylation of ERK, NF- κ B DNA binding, and iNOS mRNA levels were determined in the liver of control rats and animals subjected to a diet enriched with 3% (wt/wt) carbonyl-iron. These results were correlated with changes in liver NOS activity and parameters related to oxidative stress.

Materials and methods

Animals and treatments

Male Sprague–Dawley rats (Bioterio Central, Instituto de Ciencias Biomédicas, Facultad de Medicina, Universidad de Chile) weighing 100–150 g were housed on a 12 h light/dark cycle. Animals received a diet enriched with 3% (wt/wt) carbonyl-iron for 4–12 weeks and water ad libitum. Control animals were fed with rat chow (Champion S.A., Santiago, Chile). All animals employed received humane care according to the guidelines outlined in the Guide for the Care and Use of Laboratory Animals by the National Academy of Sciences (National Institutes of Health Publication 86-23).

Parameters related to oxidative stress

Rats were anesthetized with sodium pentobarbital (50 mg/kg ip) and the livers were perfused in situ with 140 mM KCl and 10 mM potassium phosphate buffer, pH 7.4, to remove blood. Liver protein oxidation was assayed by the reaction of 2,4-dinitrophenylhydrazine with protein carbonyls according to Reznick and Packer [19]. The results are expressed as nmol carbonyls/mg protein. The contents of hepatic reduced (GSH) and oxidized (GSSG) glutathione were determined by the

reaction by *o*-phthalaldehyde at pH 8 and 12, respectively, and results are expressed as $\mu\text{g/g}$ liver [20].

Nuclear and cytosolic extracts preparations

Nuclear protein extracts were prepared according to Deryckere and Gannon [21] from liver samples homogenized in 5 mL buffer A [containing 10 mM Hepes (pH 7.9), 0.6% Nonidet P-40 (NP-40), 150 mM NaCl, 0.5 mM phenylmethylsulfonyl fluoride (PMSF) and 1 mM *o*-vanadate] and centrifuged for 30 s at 100g and 4°C. The supernatant was incubated for 5 min on ice and centrifuged for 5 min at 700g and 4°C. The supernatant obtained corresponding to cytosolic extract was stored at -80°C and the pellet was resuspended in buffer B [containing 20 mM Hepes (pH 7.9), 25% glycerol, 420 mM NaCl, 1.2 mM MgCl_2 , 0.2 mM EDTA, 0.5 mM dithiothreitol (DTT), 0.5 mM PMSF, 2 mM benzamidine, and 5 $\mu\text{g/mL}$ of the protease inhibitors pepstatin, leupeptin, and aprotinin, incubated on ice for 20 min, and centrifuged for 30 s at 5000g and 4°C. The supernatant corresponding to nuclear extract was stored at -80°C . Protein concentration was determined by the Bradford protein assay [22].

Western blotting

The proteins of cytosolic extract were separated on a 12% SDS–PAGE [23] and transferred to a nitrocellulose membrane (Advantec MFS, USA) [24]. The phosphorylated mitogen-activated protein kinase (MAPK) p42/p44 was detected with the specific polyclonal antibody (MAPK p44/p42; Cell Signaling, Technology, MA, USA) and the non-phosphorylated MAPK p42/p44 with the specific monoclonal antibody (pan ERK; Transduction Laboratories, BD Biosciences Pharmingen, San Diego, CA, USA). Immunopure goat anti-rabbit IgG and immunopure goat anti-mouse IgG (Pierce Biotechnology, Rockford, USA) conjugated with horseradish peroxidase, were used as second antibodies, respectively, and chemiluminescent detection was made with Super-Signal West Pico Chemiluminescent kit (Pierce Biotechnology, Rockford, USA). Protein bands were quantified by densitometry analyses using ScionImage (Scion, Frederick MA, USA).

Electrophoretic mobility shift assay

Samples of nuclear extract were subjected to electrophoretic mobility shift assay (EMSA) for assessment of NF- κ B DNA binding, using oligonucleotides containing the κ B sequence in the promoter iNOS gene 5'-GCA CAC CCT ACT GGG GAC T-3' (Invitrogen Life Technologies, Carlsbad, CA, USA), labeled with [α - ^{32}P]dCTP using the Klenow DNA polymerase fragment I (Promega, Madison WI, USA). For this purpose, 8 μg

nuclear protein extract were preincubated on ice for 15 min with 10 μ L of a solution containing 2 μ L footprinting buffer [250 mM Hepes (pH 7.6), 50 mM MgCl₂ and 340 mM KCl], 3 μ L nuclear dialysis buffer [25 mM Hepes (pH 7.9), 0.1 mM EDTA, 40 mM KCl, 10% glycerol, 1 mM DTT, and 0.1 mM NaF], 0.5 μ L poly(dI:dC) (2 mg/mL), 2 μ L 0.1% NP-40, 1 μ L 150 mM NaCl, 1 μ L α^{32} P-labeled NF- κ B probe, and 0.5 μ L ultra pure water. The specificity of the reaction was confirmed in competition experiments using 100-fold excess of unlabeled DNA probe. Protein-oligonucleotide complexes were resolved using a non-denaturing 6% acrylamide gel and run in 0.5 \times TBE buffer (45 mM Tris-HCl, 45 mM boric acid, and 1 mM EDTA) for 4 h at 100 V. Gels were dried and NF- κ B bands were detected by autoradiography and quantified by densitometry using ScionImage (Scion, Frederick MA, USA). To assess the subunit composition of DNA binding protein, specific antibodies were used for supershift assay (goat and rabbit immunoglobulin-G raised against NF- κ B p50 and p65, respectively; Santa Cruz Biotechnology, Santa Cruz, CA, USA).

Reverse transcription-polymerase chain reaction (RT-PCR)

Total cellular RNA was extracted from liver samples with TRIzol reagent (Invitrogen Life Technologies, Carlsbad, CA, USA) [25]. cDNA was synthesized from total RNA using Superscript II RNase H⁻ Reverse Transcriptase (Invitrogen Life Technologies, Carlsbad, CA, USA) and random hexamer primers [pd(N)₆] (Promega, Madison, WI, USA). Synthesized cDNA was amplified using *Taq* DNA polymerase (Invitrogen Life Technologies, Carlsbad, CA, USA) in the presence of primers specific for rat iNOS. Nucleotide sequences for primers used were sense 5'-CAA CAA CAC AGG ATG ACC CTA A-3' and antisense 5'-GGT AGG TTC CTG TTG TTT CTA T-3' (Invitrogen Life Technologies, Carlsbad, CA, USA). RNA concentrations and PCR cycles were titrated to establish standard curves to document linearity and to allow semi-quantitative analysis of signal strength. To control the relative amount of iNOS mRNA transcribed in each reverse transcriptase reaction, RNA 18S invariant standards (Classic II 18S Standards (324 bp); Ambion, Austin TX, USA) were used. The products of PCR were separated on 2% agarose gels, stained with ethidium bromide, photographed, and analyzed by densitometry using ScionImage (Scion, Frederick MA, USA).

NOS activity

L-Arginine-dependent \cdot NO synthesis was measured as previously described [26], by a method in which the oxidation of oxyhemoglobin to methemoglobin by \cdot NO is monitored spectrophotometrically at 401 versus 411 nm [27]. Results are expressed as nmol \cdot NO/mg protein/min.

Protein content was assayed according to Lowry et al. [28].

Statistical analysis

Values shown are means \pm SEM for the number of separated experiments indicated. The statistical significance of differences between mean values ($p < 0.05$) was determined by one-way ANOVA and the Newman-Keuls' test (GraphPad Prism version 2.0; GraphPad software, San Diego, CA, USA).

Results

CIO enhances rat liver oxidative stress status

Formation of carbonyl derivatives of certain amino acids was used as an index of protein oxidation associated with oxidative stress [19]. Data presented in Fig. 1A show increases of 213 and 121% in the hepatic protein carbonyl content at 4 and 6 weeks after carbonyl-iron treatment compared to controls, respectively. At these experimental times, the total content of GSH (GSH + 2GSSG) was reduced by 35% in the liver of carbonyl-iron-treated rats over controls (Fig. 1B; $p < 0.05$), whereas a significant 21% diminution in the hepatic GSH/GSSG ratio was observed at 6 weeks (Fig. 1C). Accordingly, the calculated protein carbonyl/total GSH content ratio was increased by 164 and 180% at 4 and 6 weeks after carbonyl-iron enriched diet administration, respectively (Fig. 1D). CIO-induced changes in liver protein carbonyl content (Fig. 1A), total GSH content (Fig. 1B), GSH/GSSG ratio (Fig. 1C), and in the protein carbonyl/total GSH content ratio (Fig. 1D) at 4 and 6 weeks were normalized thereafter, being the values at 8–12 weeks significantly different to those found at 4 and 6 weeks, respectively.

CIO increases rat liver phosphorylation of ERK1/2

The activation of MAPK ERK1/2 was evaluated using Western blot assessment by measurements of the phosphorylated (p-ERK1/2) and non-phosphorylated (ERK1/2) forms of the enzyme. The carbonyl-iron enriched diet increased p-ERK1/2 with a respective diminution in the ERK1/2 (Fig. 2A) after 6 and 8 weeks of treatment, with significant 13- and 17-fold increases in hepatic p-ERK1/2 to ERK1/2 ratio over control values, respectively (Fig. 2B). These changes were normalized at 10 and 12 weeks after carbonyl-iron administration (Fig. 2).

CIO enhances rat liver NF- κ B binding to iNOS promoter

Transcriptional factor NF- κ B regulates the expression of iNOS [10]. To evaluate the effect of carbonyl-iron

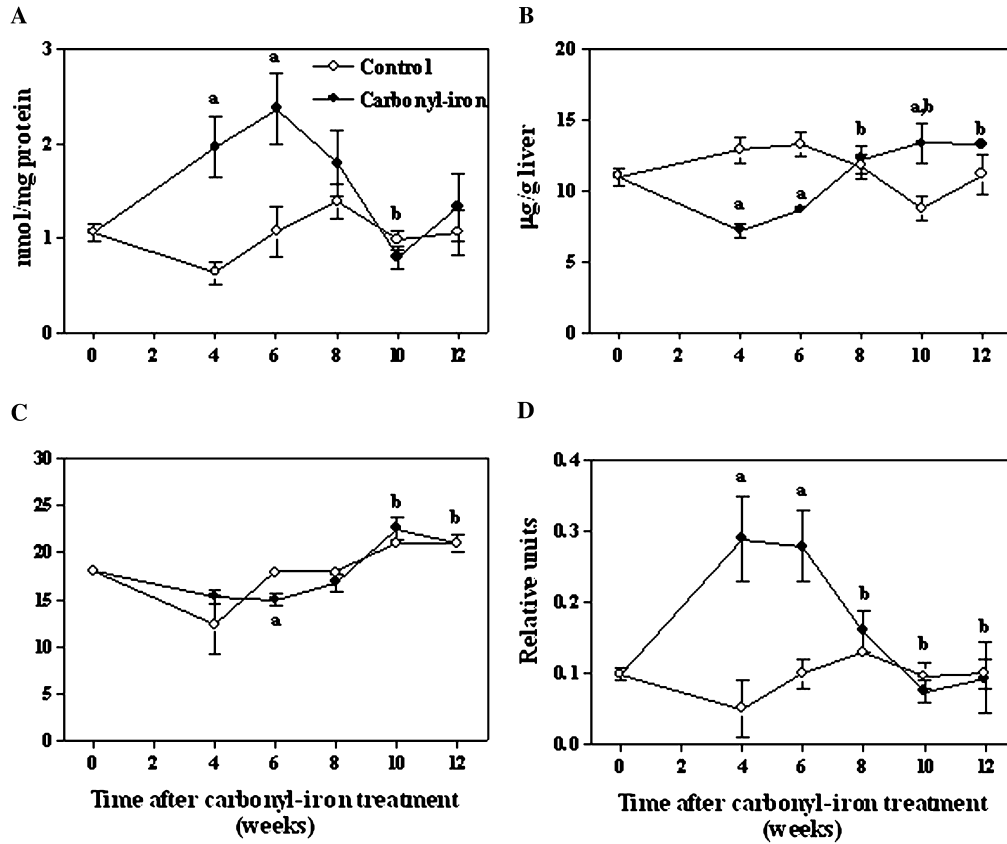


Fig. 1. Protein carbonyl content (A), total reduced glutathione (GSH) content (B), GSH/GSSG ratio (C), and protein carbonyl/total GSH content ratio (D) in the liver of control rats and carbonyl-iron-treated animals at different times after treatment. Rats were treated as described in Materials and methods. Values shown represent to means \pm SEM for 3–7 animals per experimental group. The significance of the differences between mean values was determined by one-way ANOVA and the Newman–Keuls’ post hoc test; ^a $p < 0.05$ versus control; ^b $p < 0.05$ versus iron-treated rats at 4 and 6 weeks.

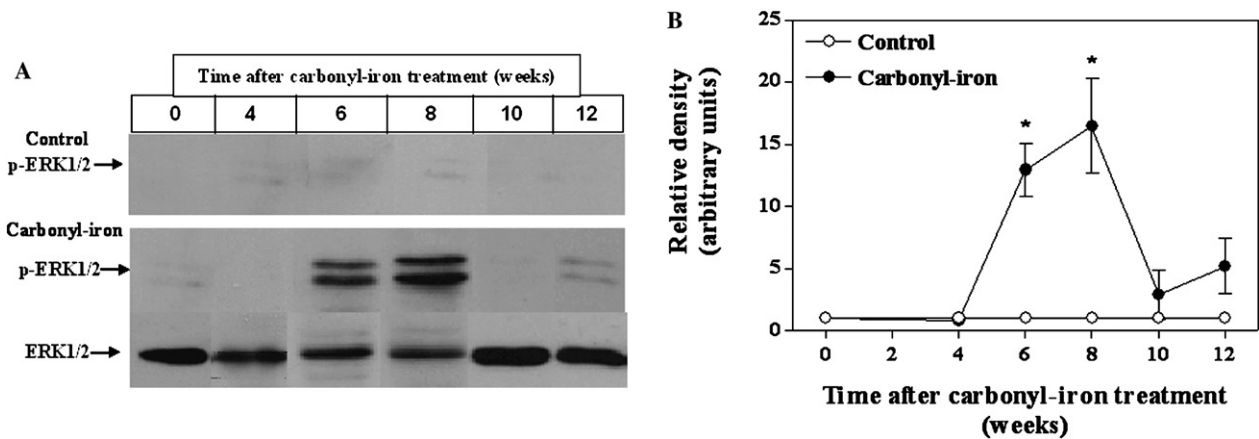


Fig. 2. Time course study of the effects of carbonyl-iron enriched diet administration on rat liver extracellular signal-regulated kinase (ERK1/2) phosphorylation. (A) Representative Western blots for phosphorylated ERK (p-ERK1/2) in cytosolic extracts from control rats and carbonyl-iron-treated animals and non-phosphorylated ERK (ERK1/2) in carbonyl-iron-treated rats at different times after treatment. (B) Densitometric quantification of p-ERK1/2 to ERK1/2 ratios in controls ($n = 3$) and carbonyl-iron-treated animals ($n = 3-6$) at different times after treatment, expressed as means \pm SEM. Mean value from control rats at time zero was arbitrarily set to unity, and values at other time points were normalized to this. Statistical analysis: $*p < 0.05$ versus controls by one-way ANOVA and the Newman–Keuls’ post hoc test.

enriched diet on NF- κ B DNA binding activity and the expression of iNOS, EMSA assay with the oligonucleotide corresponding to the κ B sequence in the iNOS promoter

was used. The time course study revealed an enhancement in liver NF- κ B binding to iNOS promoter (Fig. 3A), with a maximal effect (3.5-fold increase over control values)

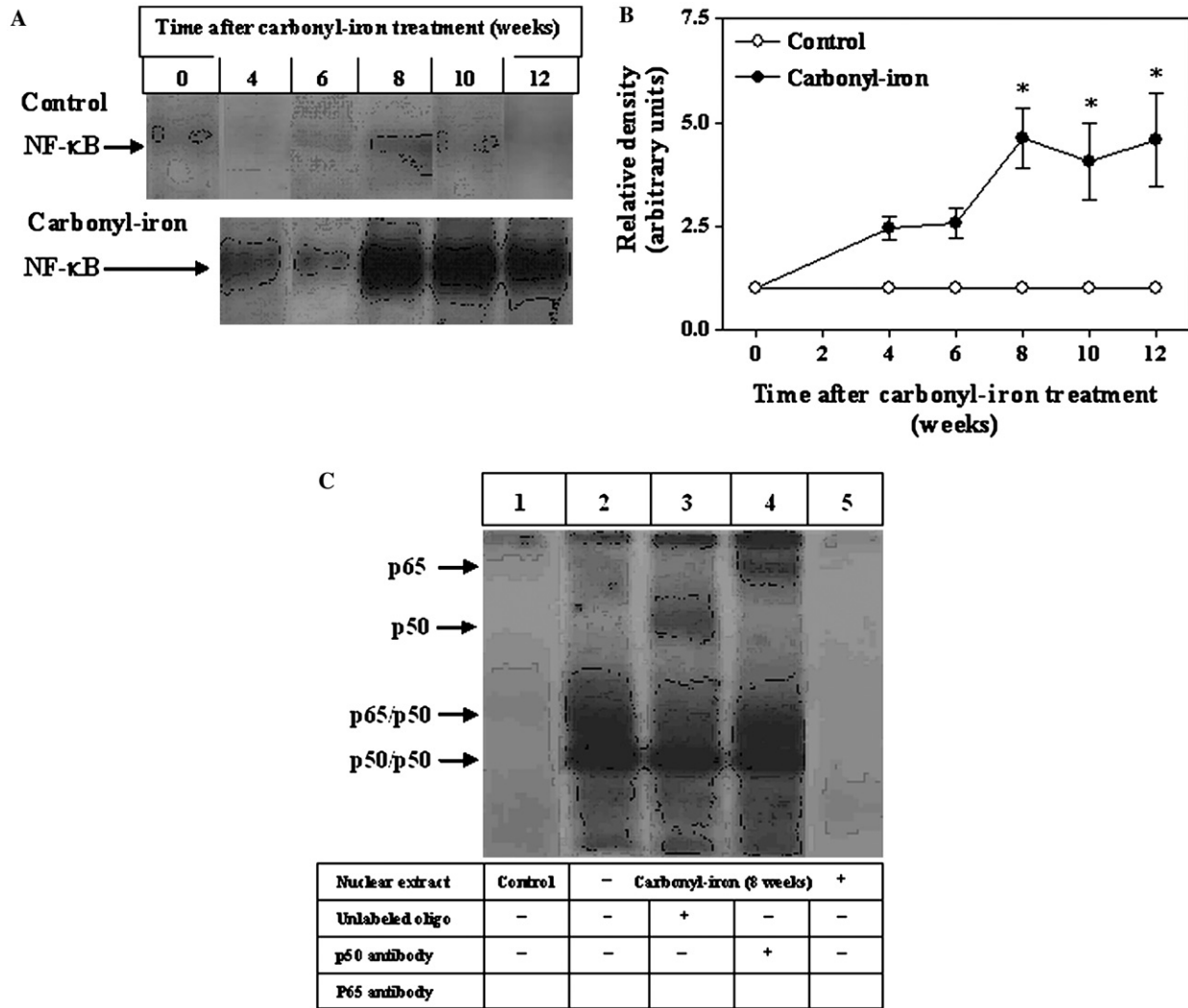


Fig. 3. Time course study of the effects of carbonyl-iron enriched diet administration on rat liver NF-κB binding to iNOS promoter. (A) Representative autoradiograph of NF-κB DNA binding activity evaluated by EMSA in nuclear extract from control rats and carbonyl-iron-treated animals at different times after treatment. (B) Densitometric quantification of relative NF-κB binding activity in controls and carbonyl-iron-treated animals at different times after treatment, expressed as means ± SEM. Mean value from control rats at time zero was arbitrarily set to unity, and values at other time points were normalized to this. Each data point represents the mean ± SEM for 3–5 different animals. Significance studies: * $p < 0.05$ versus controls by one-way ANOVA and the Newman–Keuls’ post hoc test. (C) Representative autoradiograph of NF-κB DNA binding activity evaluated by EMSA in nuclear extracts from the liver of a control rat (lane 1) and carbonyl-iron-treated animals at 8 weeks after treatment, either alone (lane 2) or under supershift analysis with antibodies specific for NF-κB p50 (lane 3) or p65 (lane 4) and in competition experiments with 100-fold excess of the unlabeled oligonucleotide (lane 5).

being observed from 8 to 12 weeks after carbonyl-iron treatment (Fig. 3B; $p < 0.05$). At 8 weeks, CIO-induced NF-κB DNA binding (Fig. 3C, lanes 1 and 2) involved the nuclear translocation of NF-κB p50 and p65 proteins (Fig. 3C, lanes 3 and 4), being the specificity of the reaction confirmed by a competition assay using a 100-fold molar excess of unlabeled DNA probe (Fig. 3C, lane 5).

CIO promotes rat liver iNOS gene expression and increases NOS activity

The pathways regulating iNOS expression seem to vary in different cells, however they usually involve

NF-κB activation [10]. CIO-induced liver NF-κB binding to iNOS promoter (Fig. 3) showed a similar time course profile to that of iNOS expression, assessed by RT-PCR (Fig. 4A), with significant 5- and 3-fold increases in the hepatic levels of iNOS mRNA being found at 8 and 12 weeks after carbonyl-iron enriched diet, compared to control values, respectively (Fig. 4B). Measurement of NOS specific activity by spectrophotometry of oxyhemoglobin oxidation to methemoglobin by ·NO [27], revealed substantial increases after carbonyl-iron administration, effects that were significant from 4 to 12 weeks of treatment over control values (Fig. 5).

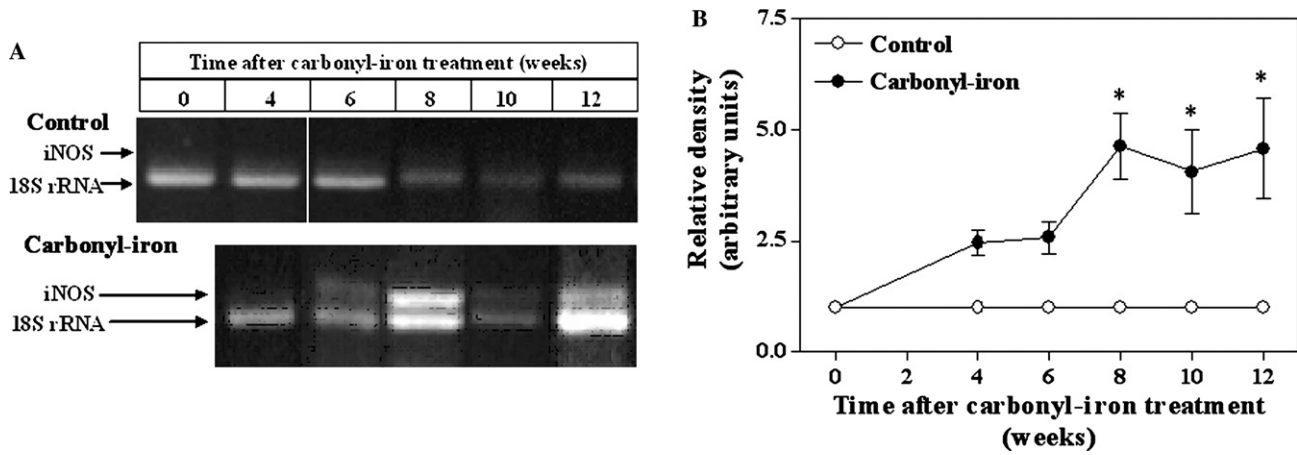


Fig. 4. Time course study of the effects of carbonyl-iron enriched diet administration on rat liver inducible nitric oxide synthase (iNOS) gene expression. (A) Representative agarose gel electrophoresis for the RT-PCR products for iNOS mRNA (417 bp) and for 18S rRNA (324 bp) after ethidium bromide staining in total hepatic RNA samples from control rats and carbonyl-iron-treated animals at different times after treatment. (B) Densitometric quantification of RT-PCR products of the mRNA of iNOS expressed as iNOS mRNA/18S rRNA ratios to compare lane-lane equivalents in total RNA content. Each data point represents the mean \pm SEM for 3–5 different animals. Data from control rats at time zero was set to unity, and values at other time points were normalized to this. Significance studies: * $p < 0.05$ versus controls by one-way ANOVA and the Newman–Keuls’ post hoc test.

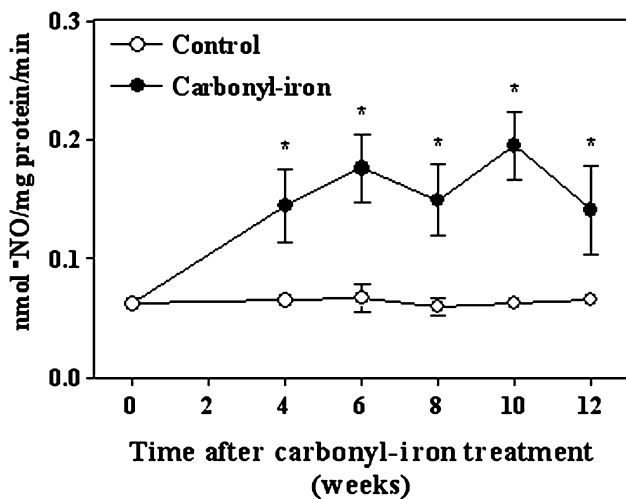


Fig. 5. Time course study of the effects of carbonyl-iron enriched diet administration on rat liver nitric oxide synthase (NOS) activity. Rats were treated as described in Materials and methods. Data shown correspond to means \pm SEM for 3–4 animals per experimental group. Significance studies: * $p < 0.05$ versus controls by one-way ANOVA and the Newman–Keuls’ post hoc test.

Discussion

Data presented confirm previous observations regarding the pro-oxidant effects of iron overload in the liver [2,3,29], as shown by the development of a biphasic oxidative stress response. This is characterized by the increase in protein carbonylation and reduction in the content of GSH as well as in the GSH/GSSG ratio of the liver observed after 6 weeks of treatment, probably induced by iron-generated free radical activity [29] and lipid peroxida-

tion by-products [8], and/or iron-dependent Kupffer cell respiratory burst activity [30]. Thereafter, the oxidative stress status induced in the liver by CIO is normalized, a change that may constitute a homeostatic response preventing hepatocellular injury from accumulating iron [31]. This is related to two major adaptive changes observed under the conditions of CIO employed, namely (i) recovery of the antioxidant potential of the liver and (ii) upregulation of hepatic iNOS expression. However, other physiological mechanisms, such as reduction in the cytosolic iron labile pool due to ferritin upregulation upon chronic iron overload, cannot be discarded.

Recovery from CIO-induced liver oxidative stress at 8–12 weeks of treatment involves the normalization of GSH depletion and reduction in the GSH/GSSG ratio induced at early times. These changes may be explained in terms of upregulation of the expression of the γ -glutamylcysteine synthetase (γ -GCS) subunit genes, which are controlled by a variety of factors including oxidative stress conditions and exposure to heavy metals [32]. The γ -GCS reaction is the rate-limiting step for GSH biosynthesis and regulation of its expression and activity is critical for cellular GSH homeostasis [32]. In addition, adequate operation of γ -GCS and glutathione reductase is needed to maintain the GSH/GSSG ratio, an important indicator of the prevailing redox environment [33].

Concomitantly with the attainment of GSH homeostasis at 8–12 weeks of CIO, liver iNOS expression is upregulated. Within this experimental period, total hepatic NOS activity is significantly elevated, an effect that is paralleled by (i) higher p-ERK1/2 to ERK1/2 ratios found at 6 and 8 weeks of CIO, (ii) increased NF- κ B binding to the iNOS gene promoter at 8–12 weeks, and (iii) higher iNOS mRNA expression at 8 and 12 weeks. These findings sug-

gest that upregulation of liver iNOS expression by CIO involves the activation of a cascade initiated by ERK1/2, a member of the family of MAPK that contribute to the transcriptional activity of NF- κ B, among other protein kinase systems [6,34]. Considering that both ERK1/2 and NF- κ B are activated under different oxidative stress conditions [6–8,34], ROS generated at early times of CIO may constitute costimulatory signals towards upregulation of liver iNOS expression at later times. Under these conditions, activation of ERK1/2 by CIO may also involve nitrosylation of cysteine 118 of p21^{ras} [35], which triggers both guanine nucleotide exchange and the activation of several members of the MAPK family including ERK1/2 [36]. \cdot NO is currently considered as a fundamental intercellular and intracellular signaling molecule essential for the maintenance of homeostasis [11], which is synthesized in the liver by different NOS isoforms, being iNOS responsible for a greater \cdot NO production upon induction [9,26,27]. Therefore, upregulation of liver iNOS by CIO may exert a hepatoprotective function, as high levels of \cdot NO can accomplish (i) the scavenging of lipid peroxyl and alkoxyl radicals, thus inhibiting lipid peroxidation [37], (ii) the interaction with iron-centers during iron-catalyzed processes either by chelation of redox-active iron [38] and/or reduction of oxoferryl species [39], thus diminishing free radical activity, and (iii) the downregulation of iron-containing proteins by coordinate translational regulatory mechanisms [11], thus decreasing the susceptibility to oxidative stress [40]. In addition to these antioxidants mechanisms, \cdot NO levels generated by CIO-induced iNOS may limit prolonged NF- κ B activation and its pro-inflammatory consequences [41], by nitrosylation of cysteine 62 of NF- κ B p50 protein that reduces DNA binding [42]. However, this proposal seems to require CIO for periods longer than the 12 weeks used in this study, as iron-induced NF- κ B activation may involve coordinate activation of multiple kinase pathways, in addition to ERK, whose extent and duration determine the persistence of NF- κ B DNA binding activity [34].

Collectively, data presented indicate that CIO triggers oxidative stress in the liver at early times, with activation of the ERK pathway and higher NF- κ B DNA binding and transcription of the iNOS gene at later times, thus supporting increased hepatic NOS activity. In line with these findings, addition of micromolar concentrations of iron to cultured Kupffer cells has been found to activate NF- κ B and tumor necrosis factor- α promoter activity, through enhancement of I κ B kinase activity [43]. Liver iNOS upregulation and the recovery of GSH homeostasis are proposed as hepatoprotective mechanisms against CIO-induced pro-oxidant effects, thus in agreement with the lack of significant hepatic histologic changes reported for this carbonyl-iron loaded rat model [44]. Although enhancement in liver NOS activity at 8–12 weeks of CIO involves iNOS upregulation, that observed after 4–6 weeks of treatment is independent of gene

expression and could be the result of a direct influence of iron on the enzyme [13]. The latter view is supported by the 100% enhancement in hepatic \cdot NO generation observed (i) 4 h after the administration of a single dose of 200 mg iron/kg and (ii) following the in vitro addition of 1 μ mol iron/mg protein to liver cytosolic fractions [13].

Acknowledgments

This work was supported by Grant 1030499 from FONDECYT (Chile). The authors thank Professor Ramón Rodrigo and Mr. Diego Soto for their assistance in glutathione measurements. Professor Felipe Sierra kindly supplied ERK1/2 antibodies.

References

- [1] D. Boldt, New perspectives on iron: an introduction, *Am. J. Med. Sci.* 318 (1999) 207–212.
- [2] S. Aust, L. Morehouse, C. Thomas, Role of metals in oxygen radical reactions, *J. Free Radic. Biol. Med.* 1 (1985) 3–25.
- [3] B.R. Bacon, R.S. Britton, The pathology of hepatic iron overload: a free radical-mediated process? *Hepatology* 11 (1990) 127–137.
- [4] P. Klatt, S. Lamas, Regulation of protein function by S-glutathiolation in response to oxidative and nitrosative stress, *Eur. J. Biochem.* 267 (2000) 4928–4944.
- [5] H. Tsukamoto, M. Lin, The role of Kupffer cells in liver injury, in: E. Wisse, D.L. Knook, C. Balabaud (Eds.), *Cells of the Hepatic Sinusoid, The Kupffer Cell Foundation*, Leiden, Netherlands, 1997, pp. 244–250.
- [6] J.L. Martindale, N.J. Holbrook, Cellular responses to oxidative stress: signaling for suicide and survival, *J. Cell. Physiol.* 192 (2002) 1–15.
- [7] V.J. Thannickal, B.L. Fanburg, Reactive oxygen species in cell signaling, *Am. J. Lung Cell. Mol. Physiol.* 279 (2000) L1005–L1028.
- [8] G. Poli, G. Leonarduzzi, F. Biasi, E. Chiarotto, Oxidative stress and cell signaling, *Curr. Med. Chem.* 11 (2004) 1163–1182.
- [9] W. Alderton, C. Cooper, R. Knowles, Nitric oxide synthases: structure, function and inhibition, *Biochem. J.* 357 (2001) 593–615.
- [10] H. Kleinert, A. Pautz, K. Linker, P. Schwarz, Regulation of the expression of inducible nitric oxide synthase, *Eur. J. Pharmacol.* 500 (2004) 255–266.
- [11] V.E. Kagan, A.V. Kozlov, Y.Y. Tyurina, A.A. Shvedova, J.C. Yalowich, Antioxidant mechanisms of nitric oxide against iron-catalyzed oxidative stress in cells, *Antioxid. Redox Signal.* 3 (2001) 189–202.
- [12] M. Galleano, M. Simontacchi, S. Puntarulo, Nitric oxide and iron: effect of iron overload on nitric oxide production in endotoxemia, *Mol. Aspects Med.* 25 (2004) 141–154.
- [13] P. Cornejo, G. Tapia, S. Puntarulo, M. Galleano, L.A. Videla, V. Fernández, Iron-induced changes in nitric oxide and superoxide radical generation in rat liver after lindane or thyroid hormone treatment, *Toxicol. Lett.* 119 (2001) 87–93.
- [14] S. Hussain, K. Raja, P. Amstad, M. Sawyer, L. Trudel, G. Wogan, L. Hofseth, P. Shields, T. Billiar, C. Trautwein, T. Höhler, P. Galle, D. Phillips, R. Markin, A. Marrogi, C. Harris, Increased p53 mutation load in nontumorous human liver of Wilson disease and hemochromatosis: oxyradical overload diseases, *Proc. Natl. Acad. Sci. USA* 97 (2000) 12770–12775.

- [15] L. Chen, B. Zhang, D. Harris, Evidence suggesting that nitric oxide mediates iron-induced toxicity in cultured proximal tubule cells, *Am. J. Physiol.* 274 (1998) F18–F25.
- [16] L. Chen, Y. Wang, L. Kairaitis, B. Zhang, D. Harris, Molecular mechanisms by which iron induces nitric oxide synthesis in cultured proximal tubule cells, *Exp. Nephrol.* 9 (2001) 198–204.
- [17] X. Zhou, Z. Laszik, X. Wang, F. Silva, N. Vaziri, Association of renal injury with increased oxygen free radical activity and altered nitric oxide metabolism in chronic experimental hemosiderosis, *Lab. Invest.* 80 (2000) 1905–1914.
- [18] A. Hida, T. Kawabata, Y. Minamiyama, A. Mizote, S. Okada, Saccharated colloidal iron enhances lipopolysaccharide-induced nitric oxide production in vivo, *Free Radic. Biol. Med.* 34 (2003) 1426–1434.
- [19] A. Reznick, L. Packer, Oxidative damage to proteins: spectrophotometric method for carbonyl assay, *Methods Enzymol.* 233 (1994) 357–363.
- [20] P. Hissin, R. Hilf, A fluorometric method for determination of oxidized and reduced glutathione in tissues, *Anal. Biochem.* 74 (1976) 214–226.
- [21] F. Deryckere, F.A. Gannon, A one-hour minipreparation technique for extraction of DNA-binding proteins from animal tissues, *BioTechniques* 16 (1994) 405.
- [22] M. Bradford, A rapid and sensitive method for the quantitation of microgram quantities of protein utilizing the principle of protein-dye binding, *Anal. Biochem.* 72 (1976) 248–254.
- [23] U.K. Laemmli, Cleavage of structural proteins during the assembly of the head of bacteriophage T₄, *Nature* 227 (1970) 680–685.
- [24] H. Towbin, T. Staehelin, J. Gordon, Electrophoretic transfer of proteins from polyacrylamide gels to nitrocellulose sheets: procedure and some applications, *Proc. Nat. Acad. Sci. USA* 76 (1979) 4350–4354.
- [25] P. Chomczynski, N. Sacchi, Single-step method of RNA isolation by acid guanidinium thiocyanate-phenol-chloroform extraction, *Anal. Biochem.* 162 (1987) 156–159.
- [26] V. Fernández, P. Cornejo, G. Tapia, L.A. Videla, Influence of hyperthyroidism on the activity of liver nitric oxide synthase in the rat, *Nitric Oxide Biol. Chem.* 1 (1997) 463–468.
- [27] R. Knowles, M. Merret, M. Salter, S. Moncada, Differential induction of brain, lung and liver nitric oxide synthase by endotoxin in the rat, *Biochem. J.* 270 (1990) 833–836.
- [28] O.H. Lowry, N.J. Rosebrough, A.L. Farr, R.J. Randall, Protein measurement with the Folin phenol reagent, *J. Biol. Chem.* 193 (1951) 265–275.
- [29] A. Pietrangelo, Iron-induced oxidant stress in alcoholic liver fibrogenesis, *Alcohol* 30 (2003) 121–129.
- [30] G. Tapia, P. Troncoso, M. Galleano, V. Fernández, S. Puntarulo, L.A. Videla, Time course study of the influence of acute iron overload on Kupffer cell functioning and hepatotoxicity assessed in the isolated perfused rat liver, *Hepatology* 27 (1998) 1311–1316.
- [31] J.W. Eaton, M. Qian, Molecular bases of cellular iron toxicity, *Free Radic. Biol. Med.* 32 (2002) 833–840.
- [32] O.W. Griffith, Biologic and pharmacologic regulation of mammalian glutathione synthesis, *Free Radic. Biol. Med.* 27 (1999) 922–935.
- [33] F.Q. Schafer, G.R. Buettner, Redox environment of the cell as viewed through the redox state of the glutathione disulfide/glutathione couple, *Free Radic. Biol. Med.* 30 (2001) 1191–1212.
- [34] Y.M.W. Janssen-Heininger, M.E. Poynter, P.A. Baeuerle, Recent advances towards understanding redox mechanisms in the activation of nuclear factor κ B, *Free Radic. Biol. Med.* 28 (2000) 1317–1327.
- [35] H.M. Lander, D.P. Hajjar, B.L. Hempstead, U.A. Mirza, B.T. Chait, S. Campbell, L.A. Quilliam, A molecular redox switch on p21^{ras}. Structural basis for the nitric oxide-p21^{ras} interaction, *J. Biol. Chem.* 272 (1997) 4323–4326.
- [36] H.M. Lander, A.T. Jacovina, R.J. Davis, J.M. Tauras, Differential activation of mitogen-activated protein kinases by nitric oxide-related species, *J. Biol. Chem.* 271 (1996) 19705–19709.
- [37] H. Rubbo, R. Radi, M. Trujillo, R. Telleri, B. Kalyanaram, S. Barnes, M. Kirk, B.A. Freeman, Nitric oxide regulation of superoxide and peroxynitrite-dependent lipid peroxidation. Formation of novel nitrogen-containing oxidized lipid derivatives, *J. Biol. Chem.* 269 (1994) 26066–26075.
- [38] J. Kanner, S. Harel, R. Granit, Nitric oxide as an antioxidant, *Arch. Biochem. Biophys.* 289 (1991) 130–136.
- [39] N.V. Gorbunov, J.C. Yalowich, A. Gaddam, P. Thampatty, V.B. Ritov, E.R. Kissin, N.M. Elsayed, V.E. Kagan, Nitric oxide prevents oxidative damage produced by tert-butyl hydroperoxide in erythroleukemia cells via nitrosylation of heme and non-heme iron. Electron paramagnetic resonance evidence, *J. Biol. Chem.* 272 (1997) 12328–12341.
- [40] J.B. Domachowski, S.P. Rafferty, N. Singhanian, M. Mardiney III, H.L. Malech, Nitric oxide alters the expression of gamma-globin, H-ferritin, and transferrin receptor in human K562 cells at the posttranscriptional level, *Blood* 88 (1996) 2980–2988.
- [41] K.R. Walley, T.E. McDonald, Y. Higashimoto, S. Hayashi, Modulation of proinflammatory cytokines by nitric oxide in immune acute lung injury, *Am. J. Respir. Crit. Care Med.* 160 (1999) 698–704.
- [42] A. Dela Torre, R.A. Schroeder, P.C. Kuo, Alteration of NF- κ B p50 DNA-binding kinetics by S-nitrosylation, *Biochem. Biophys. Res. Commun.* 238 (1997) 703–706.
- [43] H. She, S. Xiong, M. Lin, E. Zandi, C. Giulivi, H. Tsukamoto, Iron activates NF- κ B in Kupffer cells, *Am. J. Physiol. Gastrointest. Liver Physiol.* 283 (2002) G719–G726.
- [44] G.A. Ramm, Animal models of iron overload based on excess exogenous iron, in: J.C. Barton, C.Q. Edwards (Eds.), *Hemochromatosis. Genetics, Pathophysiology, Diagnosis, and Treatment*, Cambridge University Press, New York, 2000, pp. 494–507.